

Radial Electric Fields during L -to- H Transition and Edge-Localized Modes from Charge-Exchange Diagnostics of Ripple-Trapped Particles

Winfried Herrmann and Asdex Upgrade Team

Max-Planck-Institut für Plasmaphysik—EURATOM Association, D-85748 Garching, Germany

(Received 13 March 1995)

Neutral fluxes from charge-exchange processes with ripple-trapped particles depend on radial electric fields. Their time behavior during L -to- H transition and edge-localized modes (ELMs) was studied with a time resolution of up to $50\ \mu\text{s}$. No jumps at the L -to- H transition are observed that are faster than the increase of the field after ELMs. The signature of the neutral particle spectra is different for L and H modes and allows discrimination of the modes. ELMs and electric fields are present during the CDH (completely detached H) mode.

PACS numbers: 52.20.Dg, 52.25.Tx, 52.70.Nc

Since the discovery of the H mode in ASDEX [1] many ideas have been published in an attempt to explain why the plasma switches from the low-confinement L mode to the high-confinement H mode and which plasma properties are of importance in this bifurcation process. For an intensive discussion and a list of references, see, for example, Refs. [2,3]. The interest in this question derives its importance from the fact that the achievement of the H mode is fundamental to the present-day concepts of a fusion reactor. A physical understanding of the processes involved would put extrapolations on a safer basis.

One of the main ingredients in many theories about the L -to- H transition is the development and behavior of a radial electric field at the edge of the plasma [4–6], whose shear could suppress fluctuations [7–9] and explain the improvement of confinement in H mode by the development of a heat conduction and particle diffusion barrier. Electric fields perpendicular to a magnetic flux surface have been measured, especially on DIII-D, from the poloidal rotation of impurity ions [10–12], as well as of the basic plasma constituent [11].

These measurements show a distinct difference in the electric field profiles in the L and H modes. The electric field is negative in H mode, with a level of shear sufficient to suppress fluctuations. The time resolution of these spectroscopic measurements seems to be limited to not much less than a millisecond. To shed more light on and eventually decide on the causality in the L -to- H transition, better time resolutions are essential. Surprisingly, it turns out, and this will be the subject of this Letter, that fluxes from neutrals that result from charge exchange (CX) with slowing-down ions from neutral injection and that have scattered into the ripple-trapped domain can contain information about electric fields in the plasma. The time resolution of a flux measurement can be shorter than $100\ \mu\text{s}$, the limitation resulting from the analyzer counting capability and from the intrinsic time scale of the particle trajectories in the plasma.

A CX analyzer of ASDEX Upgrade was set to detect neutrals, which belong to the class of mirror-trapped particles before charge exchange. Because of the fast grad B drift of energetic particles, these orbits should be almost unpopulated in the plasma. Only after the development of perpendicular electric fields could they remain in the plasma and, after charge exchange, be detected by the analyzer. Times to scatter particles from banana orbits to mirror-trapped orbits are in the range of $100\ \mu\text{s}$.

A description of the measuring system will be given in a more detailed publication. The analyzer is one of the devices built for Joint European Torus (JET) by the Frascati Laboratory [13] Figure 1 shows signals of D_α light and neutral fluxes for an ASDEX Upgrade shot for a time window around the L -to- H transition. The uppermost trace is the D_α signal, which usually serves for discrimination of the modes. At 1.6 s a deuterium heating beam with about 2.6 MW is injected into a deuterium plasma with a current of $I = 1000\ \text{kA}$ and a central field of $B = -2.1\ \text{T}$ (drift towards the X point). The acceleration voltage of the beam is $62\ \text{kV}$.

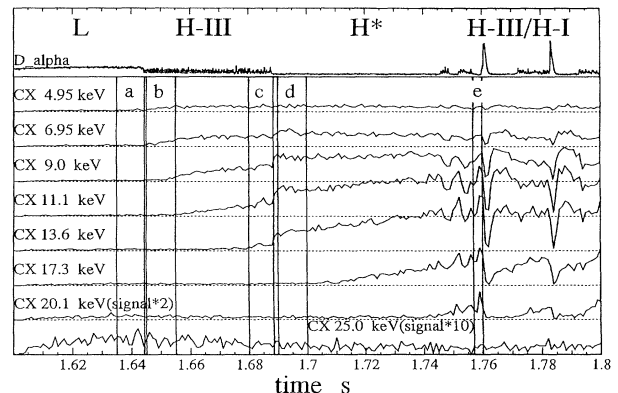


FIG. 1. D_α and neutral fluxes at different energies around the time of transition from L to H mode with $1\ \text{ms}$ time resolution. Time slices a – e are intervals in which energy spectra of Fig. 5 were made.

and the injected power fraction in full, half, and one-third injection energy is about 60%, 17%, and 23%. The slowing-down time of the full energy ions lies in the range of 10 ms. The average plasma density increases from $\bar{n} = 4.5 \times 10^{19} \text{ m}^{-3}$ in *L* mode to $\bar{n} = 6.7 \times 10^{19} \text{ m}^{-3}$ in *H* mode. The poloidal ion gyroradius is less than 1 cm at the plasma edge. The plasma transits from *L* to *H* mode at 1.644 s, develops some noisy pattern—probably nonresolved type-III ELMs or dither—and enters a quiescent *H** mode at about 1.688 s. The first type-I ELM appears at 1.760 s.

The other traces in the figure show eight channels of the CX analyzer for the neutral energies given at the left side of the figure. After injection of the beam the signal level increases but reaches a stationary low value during *L* mode. After the transition the signal level again starts to increase, the earlier the lower the energy of the neutrals. In a broad energy range the fluxes show a “jump,” which later will be shown to be an artifact, at the transition to the quiet *H** phase. The flux of the 20.1 keV neutrals increases only shortly before the first ELMs. During the ELMs the fluxes of the particles with the higher (nonthermal) energies reduce to about the signal level in *L* mode.

The flux of neutral particles $F(E)$ is determined by the following relation

$$F(E) = k(E) \int n_i(E, r) n_0(r) \eta(E, r) dr,$$

where $k(E)$ takes into account geometrical factors, the charge exchange rate and sensitivity factors of the analyzer, $n_i(E, r)$ is the density of slowing-down particles of energy E at minor radius r in a phase space seen by the analyzer, $n_0(r)$ is the local neutral density, and $\eta(E, r)$ the penetration probability of the neutrals through the plasma to the analyzer. There are two distinct possibilities for changes in F : reaction of n_i, n_0, η to changes in the plasma density n_e and plasma temperature T , and the change of n_i due to changing orbit effects under the influence of an electric field. A correct estimate of the first possibility should take into account the spatial deposition and slowing down of the injected neutral beam as a function of n_e and T together with the dependence of n_0 and η on these parameters. Full information on these quantities is difficult to get. Rough estimates show that density and temperature variations in the *L*-to-*H* transition and during ELMs could explain a factor of about 2 in the fluxes. The fact that the flux of the slowing-down particles increases after the transition contradicts the expectation based on the increased ion and electron densities and consequently reduced neutral density. The changes in fluxes can be an order of magnitude larger than estimated above. In addition, the change of the fluxes is not the same for different energies, as would be expected for changes in plasma background.

These drastic changes in the fluxes can, however, be explained if an electric field, perpendicular to the flux

surfaces is assumed in the neighborhood of the separatrix. Single particle calculations show that ripple-trapped ions, that are lost due to the grad B drift in about 50 μs without electric field, are confined, if an electric field similar in shape to the one measured in DIII-D [14] is applied for an ASDEX Upgrade geometry and if the field strength is larger than 1 kV/m for 1 keV of ion energy. The general effect of electric fields on loss trajectories was treated in Ref. [15].

Calculations of the heating beam deposition and of the trajectories of the injected neutral beam deuterons show that a large fraction of them is concentrated at the outer part of the plasma, where the field ripple is effective.

These considerations lead us to conclude that the main structures of the CX signal, as shown in Fig. 1, are caused by a radial electric field. This grows steadily after the *L*-to-*H* transition with a jump at the transition to the quiet *H**-phase. There is no indication for a jump at the *L*/*H*-transition.

If the early phase after a *L*-to-*H* transition is observed with 50 μs time resolution (Fig. 2), one can see that ions up to 10.8 keV are affected by type-III ELMs: during the ELM the field is reduced. The field between ELMs grows in time and the last type-III ELMs influence fluxes at 13.3 keV. The jump in Fig. 1 at the transition to the quiescent *H** phase turns out to be a result of integration over the type-III ELMs. Figures 1 and 2 then indicate a steady growth of the electric field interrupted by ELMs. The fastest increase in field strength—jump—occurs at the recovery of the field after ELMs and is of the order of 10^8 V/m/s .

Figure 3 shows the *L*-to-*H** transition with positive toroidal field (unfavorable drift direction away from the *X* point). The electric field “jumps” in this case without type-III ELMs at the transition and then continues to grow. This jump lasts for about 1 ms and is not faster than the increase of the field after a type-III ELM. To clarify the picture of the *L*-to-*H* transition with favorable

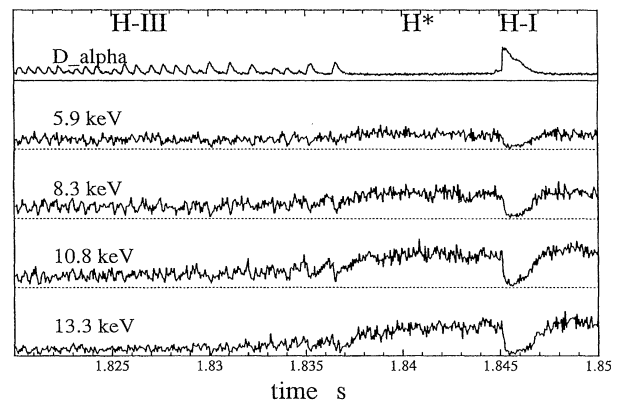


FIG. 2. D_α and neutral fluxes during a type-III ELM phase with 50 μs time resolution.

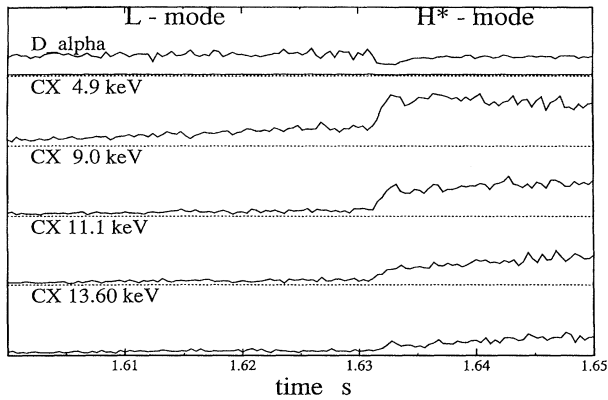


FIG. 3. D_α and neutral fluxes for a transition from L to a quiet H^* phase with $400 \mu\text{s}$ time resolution.

field direction measurements with optimized setting of the analyzer are needed to reduce statistical fluctuations at high time resolution, necessary to resolve type-III ELMs. Presently available measurements show no clear jumps in the particle fluxes at the L -to- H transition but a field that is growing afterwards with a longer (100 ms) time constant. No indications were observed up to now for any action in the fluxes prior to the L -to- H transition.

Figure 4 compares the fluxes at 11.1 keV (dotted line) with a time resolution of $100 \mu\text{s}$ during an ELM with the (inverted) D_α signal (time resolution $25 \mu\text{s}$, full line). The flux and hence the electric field decays in a time of less than or about $100 \mu\text{s}$. Obviously there is no action of the electric field prior to the steep increase in D_α .

Because of the electric field the energy spectra of neutrals originating from ripple-trapped ions develop specific shapes for the different modes of the plasma. In Fig. 5 the different spectral curves represent different modes and different development stages of the modes for the shot. The time slices, for which spectra are taken, are labeled *a* to *e* and are marked in Fig. 1. Like Fig. 1 this figure shows that the electric field grows in time and confines ripple-trapped particles with increasing energy. The low-energy points represent particles from the background plasma. The increase of their fluxes in time is related to the increase in plasma density and possibly also neutral density, connected with neutral injection. According to single particle calculations curve *e* suggests that the electric field has reached a value in the range of 20 kV/m. The form of the curves in Fig. 5 is a representative signature of the plasma mode. Especially curves *a* and *e* can be taken as signature for the L and H modes.

It is also interesting to study the shape of the spectra during type-I ELMs. In Fig. 6 the energy spectra are plotted at different time slices during an ELM, indicated in Fig. 4. The signature of the spectra at the start of the

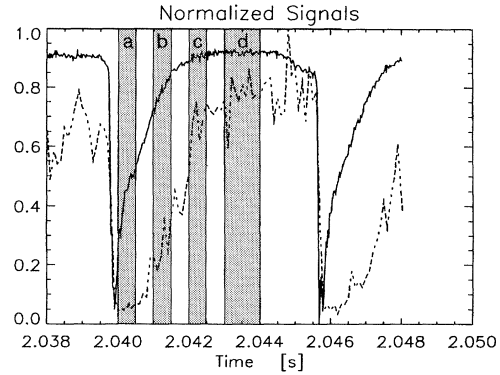


FIG. 4. Solid line: D_α signal (inverted, $25 \mu\text{s}$ time resolution); dotted line: CX signal for 11.2 keV particles ($100 \mu\text{s}$ time resolution).

ELM and after the end of it are obviously the signatures of the L and H modes. The conclusion that the type-I ELMs revert to L mode may be overinterpreting the data. It seems undoubtful, however, that the radial electric field after the beginning of an ELM falls to low levels observed in L mode.

The signature of the slowing-down particles undoubtedly determines the mode of the plasma, when the D_α diagnostic does not give clear mode identification as in the CDH (completely detached H) phases [16]. This also indicates that the radial electric fields persist in these phases. That also the ELMs persist in CDH phases can be seen from the correlation of the fluctuations in the fluxes for different energies. Although the high frequency of the ELMs in these cases prevented their resolution in time, common aliasing effects in the fluxes lead to correlation in the fluxes if ELMs are present. The correlation analysis gives mode identification consistent with that from the spectral signature and other diagnostics.

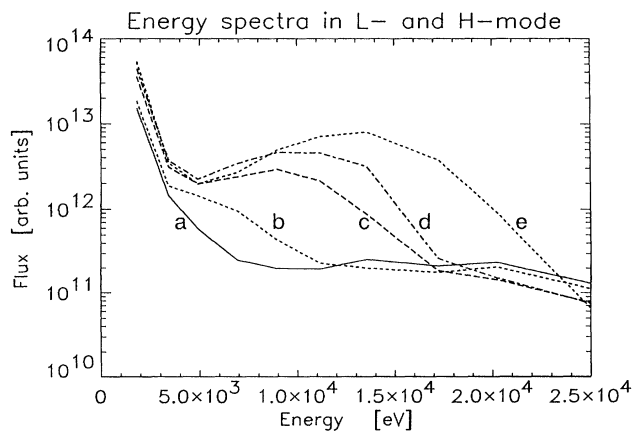


FIG. 5. Energy spectra for different phases of the L -to- H transition for time slices marked *a* to *e* in Fig. 1.

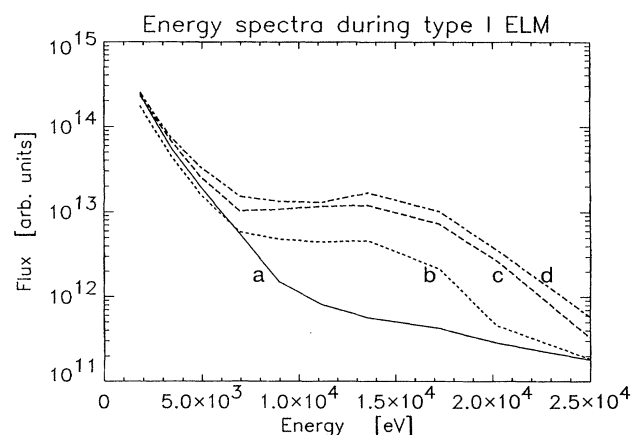


FIG. 6. Energy spectra during an ELM for time slices marked *a* to *d* in Fig. 4.

The discrimination of modes is an interesting practical side effect on the action of the electric field. In the main question of discrimination of the theoretical models underlying the *L*-to-*H* transition the presented experimental results are in favor of theories that do not need an electric field as an active element for the *L*-to-*H* transition.

The work of Dr. H.-U. Fahrbach in running the CX analyzer and discussions with Professor M. Kaufmann, Professor K. Lackner, Dr. F. Ryter, Dr. H. Zohm, and many colleagues are gratefully acknowledged.

- [1] F. Wagner *et al.*, Phys. Rev. Lett. **49**, 1408 (1982).
- [2] K. H. Burrell *et al.*, Phys. Plasmas **1**, 1536 (1994).
- [3] J. Hugill, Plasma Phys. Controlled Fusion **36**, B173 (1994).
- [4] K. C. Shaing and E. C. Crume, Jr., Phys. Rev. Lett. **63**, 2369 (1989).
- [5] R. J. Taylor *et al.*, Phys. Rev. Lett. **63**, 2365 (1989).
- [6] S.-I. Itoh and K. Itoh, Phys. Rev. Lett. **60**, 2276 (1988).
- [7] H. Biglari, P. H. Diamond, and P. W. Terry, Phys. Fluids B **2**, 1 (1990).
- [8] K. C. Shaing, E. C. Crume, Jr., and W. A. Houlberg, Phys. Fluids B **2**, 1492 (1990).
- [9] H. Matsumoto *et al.*, Plasma Phys. Controlled Fusion **34**, 615 (1992).
- [10] R. J. Groebner, K. H. Burrell, and R. P. Seraydarian, Phys. Rev. Lett. **64**, 3015 (1990).
- [11] J. Kim *et al.*, Phys. Rev. Lett. **72**, 2199 (1994).
- [12] K. Ida *et al.*, Phys. Rev. Lett. **65**, 1364 (1990).
- [13] R. Bartiromo *et al.*, Rev. Sci. Instrum. **58**, 788 (1987).
- [14] P. Gohil *et al.*, in Proceedings of the 21st European Conference on Controlled Fusion and Plasma Physics, Montpellier, France, 1994, Vol. 18b, Part II, p. 858.
- [15] M. Tendler, U. Daybelge, and V. Rozhansky, in Proceedings of the Conference on Plasma Physics and Controlled Nuclear Fusion Research, Würzburg, Germany, 1992, Vol. 2, p. 243.
- [16] M. Kaufmann *et al.*, in Proceedings of the 15th International Conference on Plasma Physics and Controlled Nuclear Fusion Research, Seville, Spain, 1994; Report No. IAEA-CN-60/A-4-I-1.